

# Investigating the Influence of Red Blood Cell Heterogeneity on Cell Transport and Blood Flow Hemodynamics

Runxin Wu<sup>1[0009-0008-1945-413X]</sup>, Mohammed Shihab Kabir<sup>1[0009-0008-1743-4581]</sup>, Aristotle Martin<sup>1[0000-0002-8704-764X]</sup>, Wentao Ma<sup>1[0000-0002-6472-3385]</sup>, and Amanda Randles<sup>1[0000-0001-6318-3885]</sup>

Dept of Biomedical Engineering, Duke University, Durham NC 27705, USA  
{wendy.wu, shihab.kabir, aristotle.martin, wentao.ma, amanda.randles}@duke.edu

**Abstract.** Red blood cell distribution width (RDW), a routinely measured biomarker of red blood cell (RBC) size heterogeneity, is strongly associated with cardiovascular events, cancer progression, and mortality. However, its mechanistic role remains poorly understood due to limited experimental control and the computational difficulty in modeling heterogeneous cell populations. Therefore, we develop and verify a high-resolution, massively parallel computational framework that explicitly models physiologically relevant RDW levels and quantifies their impact on blood flow and cell transport. Using large-scale parallel simulations across representative vascular geometries, including straight vessels, bifurcations, stenoses, and expansions, we show that bulk hemodynamics are largely insensitive to RDW variation, whereas RBC transport and circulating tumor cell (CTC) margination are strongly affected. These results highlight the importance of RBC heterogeneity in cell-level transport modeling and provide mechanistic insight into the links between RDW and disease risk. Our framework enables the scalable incorporation of patient-specific RDW into predictive simulations, supporting precision modeling in cardiovascular and oncological applications.

**Keywords:** Fluid-structure interaction · Multiscale modeling · Parallel computing · Red blood cell distribution width · Biomechanics.

## 1 Introduction

Red blood cell distribution width (RDW) is a routine clinical metric derived from complete blood counts that quantifies heterogeneity in red blood cell (RBC) morphology. Elevated RDW has emerged as a strong prognostic indicator in a wide range of diseases, including cardiovascular disorders, heart failure, and cancer progression [1, 2]. Increased RDW is associated with higher mortality in myocardial infarction, stroke, and coronary artery disease, as well as reduced survival in multiple cancers such as lung, prostate, and breast malignancies [3, 4] (Figure 1 (A,B)). RDW also correlates with tumor differentiation, volumetric growth,

and metastatic burden [5,6]. Despite these clinical associations, the mechanisms by which RDW contributes to disease progression remain unresolved.

One hypothesis suggests that RDW reflects systemic dysfunction, including chronic inflammation, oxidative stress, or nutritional deficiencies [2]. These conditions alter erythropoiesis and membrane integrity, increasing RBC size variability while simultaneously worsening disease outcomes. An alternative hypothesis suggests that RDW plays a more direct biomechanical role by altering the collective dynamics of blood flow and cell transport in the vasculature [7]. High RDW introduces heterogeneity in cell size and shape, which could influence shear stress distributions, margination behavior, and cell-wall interactions, factors known to regulate vascular health and metastatic potential.

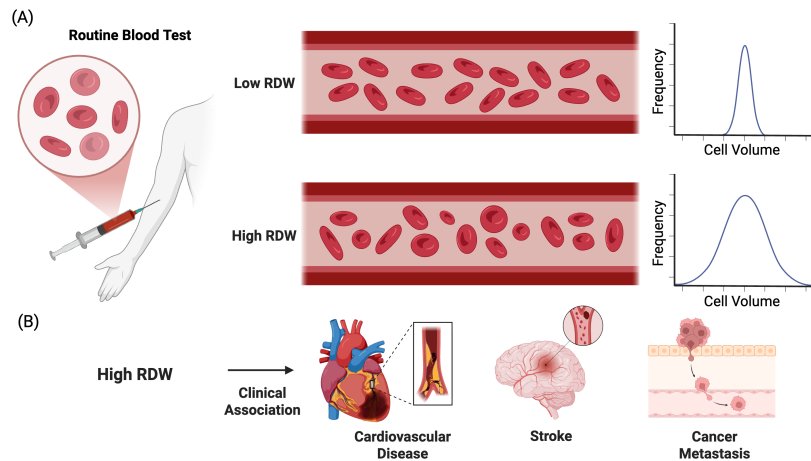


**Fig. 1. Red blood cell distribution width (RDW) physiology overview. (A).** RDW demonstration based on cell volume distribution curve: low RDW condition (below 15%), high RDW condition (above 15%). **(B).** RDW clinical association with diseases. Created in BioRender. Wu, W. (2026).<https://BioRender.com/i77i950>

However, quantifying the biomechanical influence of the heterogeneity of RBC *in vivo* is challenging due to the limited control over the properties of individual cells and the dynamic complexity of the circulatory system. Experimental models are constrained by the natural variability of human erythropoiesis and by storage-induced changes in red blood cell deformability [8,9]. Most computational studies also assumed homogeneous RBC populations, overlooking a critical source of variability in cardiovascular modeling [10–12].

To address this gap, we developed a scalable computational framework that explicitly models the heterogeneity of the size of the red blood cell to investigate its effect on blood flow and cell transport. We employed the HARVEY platform, a validated massively parallel fluid-structure interaction solver that simulates high-resolution cell mechanics coupled with fluid dynamics in large-

scale vascular flows, but yet the framework assumed identical material properties of RBCs. To study the effect of RDW, we introduced a heterogeneous RBC module in HARVEY to incorporate cell-specific morphologies and mechanical properties [13]. This model enables precise control over RDW levels in a clinically relevant range (0–40%), allowing isolation of biomechanical effects independently of systemic confounders. As a proof of concept, we simulated the transport of RBC and circulating tumor cells (CTCs) in four vascular geometries: a straight cylinder, a Y-shaped bifurcation, a stenosed artery, and an expanded microchannel. These geometries represent common anatomical and pathological features in cardiovascular and oncological contexts, where localized flow disruption and wall interactions can significantly influence disease progression [14]. We assessed how increasing RDW affects hemodynamics, including velocity, pressure, and wall shear stress, as well as cell dynamics such as force generation and margination.

Our results demonstrated that while macroscopic hemodynamics remain robust to RDW variation, cell level transport was strongly modulated by RBC heterogeneity in a geometry-dependent manner. In particular, high RDW increased the margination of circulating tumor cells by more than two-fold, providing a plausible biomechanical mechanism that links RDW to metastatic risk. By enabling detailed and scalable simulations of heterogeneous RBC populations, this work establishes a new computational framework to dissect the functional role of RDW and advance predictive modeling in cardiovascular and oncological research. From a computational science perspective, this work introduces one of the first cell-resolved blood flow frameworks that allows explicit control over population-level heterogeneity while retaining strong and weak scaling on distributed-memory systems.

## 2 Model Overview

### 2.1 Lattice Boltzmann Method for fluid transport

To enable scalable fluid simulations in complex vasculature geometries, HARVEY used the lattice Boltzmann method (LBM) to solve the Navier-Stokes equation that governs fluid dynamics. LBM is a mesoscopic approach that discretizes the domain to solve local particle advection and collision [15]. For the advancement of every time step, the  $i^{\text{th}}$  component of the probability function for the particle distribution at location  $\mathbf{x}$  at time  $t$  with velocity  $\mathbf{c}_i$  followed the lattice Boltzmann equation:

$$f_i(\mathbf{x} + \mathbf{c}_i, t + 1) = \left(1 - \frac{1}{\tau}\right) f_i(\mathbf{x}, t) + \frac{1}{\tau} f_i^{\text{eq}}(\mathbf{x}, t) + F_i(\mathbf{x}, t) \quad (1)$$

where particle collision was modeled by the Bhatnagar-Gross-Krook (BGK) operator with relaxation time  $\tau$  towards Maxwellian equilibrium  $f_i^{\text{eq}}$ .  $\tau$  was determined from the prescribed kinematic viscosity and set as 1 to stay in numerically stable range.  $F_i$  denoted external body forces from cell interaction.

## 2.2 Modeling heterogeneous RBC at target RDW level

To model the heterogeneity of the RBC size, cells were created based on the physiological range of sizes and levels of RDW. Specifically, in a healthy population, red blood cells generally have a biconcave shape with dimensions of 7.5 to 8.7 microns for the diameter of the major axes and 1.7 to 2.2 microns for the thickness of the minor axes [16]. Therefore, we placed RBCs with the mean semi-axis dimension (4, 4, 1) microns. In addition, RDW is defined as the standard deviation of the volume of red blood cells divided by the mean volume represented as a percentage [7]. Normal RDW has been observed below 15%, while a high RDW has been observed in the range between 15% and 40% in some critically ill patients [17]. To investigate the clinical range of RDW, we experimented with five targeted levels of RDW: 0%, 10%, 20%, 30%, and 40%.

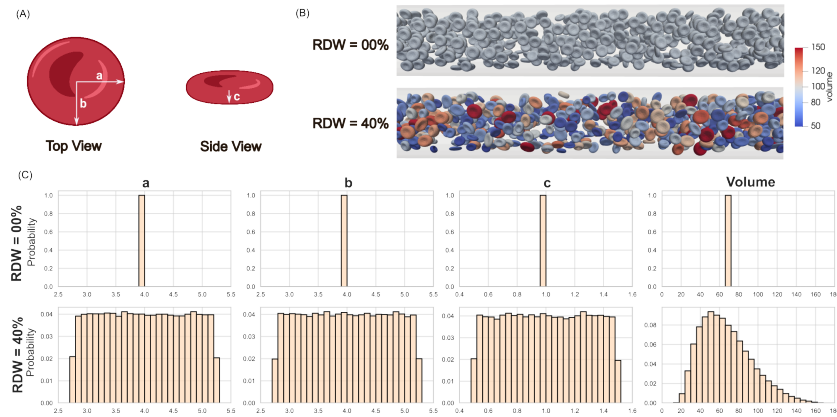


**Fig. 2. Modeling heterogeneous RBCs.** (A). Top and side view of a red blood cell, annotated by semi-axis a, b, c. (B). Cell tile illustration with RDW level 0% and 40%. (C). Distribution range of semi-axis a, b, c, and total cell volume in cell tiles of different RDW levels.

As shown in Figure 2 (A), each semi-axis of the RBC was sampled from a specified uniform random distribution. As the range of each semi-axis increases, we can control the RBC heterogeneity to reach the target RDW level. The volume distributions presented slight skewness to the left for higher RDW levels, due to the cubic power of large outliers in the axis size. Given that the overall distribution resembles the normal distribution, we assumed that slight skewness at higher RDW levels would not influence downstream analysis (Figure 2 (C)). To achieve randomness in RBC population configurations, cell packing sampled random angles and was optimized for maximum density without overlap [18]. This implementation enabled us to populate vascular geometries with randomly packed heterogeneous RBCs at the target RDW and hematocrit level (Figure 2 (B)), laying the ground for studying RBC heterogeneity in blood transport.

### 2.3 Finite Element Method for cell mechanics

Cells were modeled as viscous fluid enclosed by an elastic membrane to account for physical properties such as deformability and resistance to bending. The finite element method (FEM) is implemented to construct a Lagrangian triangular mesh for cells [19]. RBCs were modeled as biconcave shapes, while the CTCs were modeled as spheres. We used Skalak constitutive law for stress-strain relationship to calculate the elastic energy  $W_s$ , proportional to the shear modulus  $G_s$ .

$$W_s = \frac{G_s}{4}(I_1^2 + 2I_1 - 2I_2 + CI_2^2) \quad (2)$$

where  $C$  denoted the area preservation constant and  $I_1, I_2$  were the principal strains of the Green tensor. Similarly, we incorporated cell-specific original volume and reference configuration for stress-strain calculation, instead of using default cell-type information. As a consequence, the amount of memory required to hold cell information and attributes increases on individual processors.

### 2.4 Immersed Boundary Method for Fluid Structure Interaction

To achieve the two-way coupling between fluid and cells, we used the immersed boundary method (IBM). LBM, FEM, and IBM solvers are advanced within the same global time step, and the stability of the coupled scheme is ensured by using sufficiently small time steps and cell forces that do not introduce oscillations. First, we calculated the velocity of the cell  $\mathbf{V}$  in the Lagrangian cell mesh  $\mathbf{X}$  by interpolating the surrounding fluid velocities  $\mathbf{v}$  at the Eulerian grid point  $\mathbf{x}$  that fell within the range of the support function  $\delta$ .

$$\mathbf{V}(\mathbf{X}, t) = \sum_{\mathbf{x}} \mathbf{v}(\mathbf{x}, t) \delta(\mathbf{x} - \mathbf{X}(t)) \quad (3)$$

Similarly, the deformed cells then, in turn, spread the forces  $\mathbf{G}(\mathbf{X}, t)$  to the Eulerian fluid grid to obtain  $\mathbf{g}(\mathbf{x}, t)$  [20].

$$\mathbf{g}(\mathbf{x}, t) = \sum_{\mathbf{X}} \mathbf{G}(\mathbf{X}, t) \delta(\mathbf{x} - \mathbf{X}(t)) \quad (4)$$

### 2.5 Message Passing Interface for heterogeneous cell communication

Simulating such cellular-level heterogeneity within large vascular domains imposes substantial computational demands. Individual simulation performed require around 400 hours of compute time if run serially on the Duke Compute Cluster. To overcome this barrier, we implemented CPU-based parallelization, significantly reducing computation time and enabling the simulation of more complex and larger-scale vascular networks. HARVEY employed message passing interface (MPI) parallelization to decompose the vascular domain and distribute the computation to different processors. As the cells travel through the vascular geometry, the main challenge for parallelization is to maintain cell list

information in each vascular domain owned by different tasks, and effectively communicate properties of cells at the halo region [21]. In addition to cell velocity, forces, and vertex coordinates, the heterogeneous framework also exchanged original volume for penalty terms and reference configurations to ensure correct cell mechanics computation.

The heterogeneous RBC module preserves the governing equations of fluid transport and cell mechanics, with differences mainly in cell data handling and MPI communication. We verified that heterogeneous RBC routine reproduced identical solutions to the homogeneous solver for uniform cell populations at matched processor counts across all geometries. Given prior validation of the HARVEY framework against clinical fractional flow reserve and experimental measurements of velocity, wall shear stress, and cell deformation [19, 22–25], the heterogeneous extension provides physiologically relevant predictions while enabling explicit modeling of RBC heterogeneity.

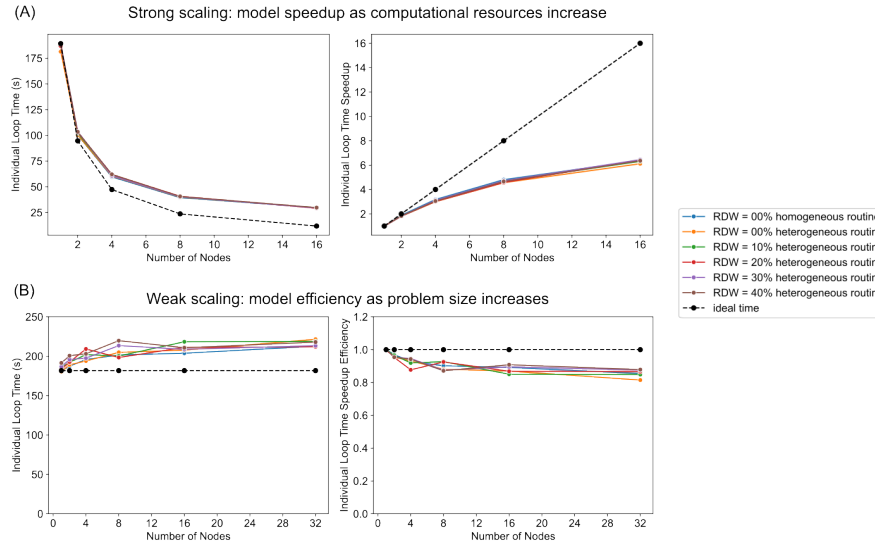


**Fig. 3. Model speedup and scaling efficiency for parallel processing of heterogeneous RBC simulations.** Dashed line represents ideal scaling. (A). Strong scaling (B). Weak scaling.

## 2.6 Model scalability and performance evaluation

To enable simulations over larger spatial domains and longer physical times, the heterogeneous routine was parallelized and evaluated on the Duke Compute Cluster using strong and weak scaling analyses. Strong scaling for a fixed 396

$\mu\text{m}$  domain across 1 to 16 nodes and RDW levels from 0 to 40 percent showed near ideal speedup at low node counts, with saturation at approximately six fold at 16 nodes due to communication overhead (Figure 3 (A)). In contrast, weak scaling achieved approximately 80 percent parallel efficiency from 1 to 32 nodes as domain size increased proportionally (Figure 3 (B)). Together, these results demonstrated robust scalability, particularly for large problem sizes, enabling high resolution, large scale vascular simulations.

Runtime comparisons showed minimal differences between the homogeneous and heterogeneous routines across all tested conditions. Despite additional cell specific computations and memory overhead, the heterogeneous implementation maintained comparable performance and introduced no new scalability bottlenecks. This demonstrated that the framework enabled explicit modeling of RBC heterogeneity at target RDW levels without prohibitive computational cost, providing a robust platform for simulating cell flow wall interactions relevant to physiological and pathological processes. Importantly, the heterogeneous formulation introduced no additional global synchronization points beyond those already present in the homogeneous solver, preserving parallel efficiency even as cell-level complexity increases.

## 2.7 Parameter selection and in Silico experiment design

To assess the impact of RDW on hemodynamics and cell transport, simulations were performed in four representative vascular geometries (Figure 4). Simulations employed a  $1\ \mu\text{m}$  lattice resolution to resolve cell scale features and ensure fluid spatial convergence, with constant inlet velocity, zero pressure outlet, and no slip rigid boundary conditions.

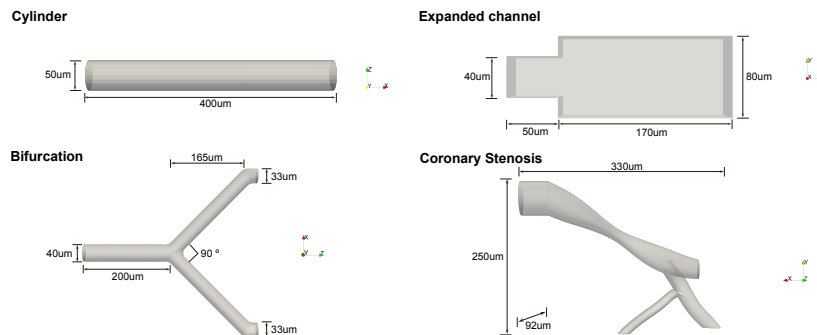


**Fig. 4. Vascular geometry employed annotated with dimensionality:** Cylinder, bifurcation, expanded channel, and coronary stenosis with vessel narrowing.

RBC-only simulations were performed in the cylinder, Y-shaped bifurcation, and stenosis geometries at an inlet velocity of  $0.01\ \text{ms}^{-1}$  at 0.1 hematocrit.

Based on power analysis with observed significance ratio, each RDW level conducted 125 simulations with randomized initial configurations to capture ensemble behavior. Fluid velocity, pressure, wall shear stress, and cell-free layer were evaluated at all lattice points, while cell velocity and force magnitude were measured at the 162 vertices per cell, with statistical differences assessed using the Wilcoxon rank-sum test at a significance level of 0.05. In the expanded channel, RBC-CTC interactions were simulated at an inlet velocity of  $0.1 \text{ ms}^{-1}$  in a converged flow with deformed RBCs [26].

### 3 Results and Discussion

#### 3.1 Geometry characteristics greatly influence hemodynamics and cell transport

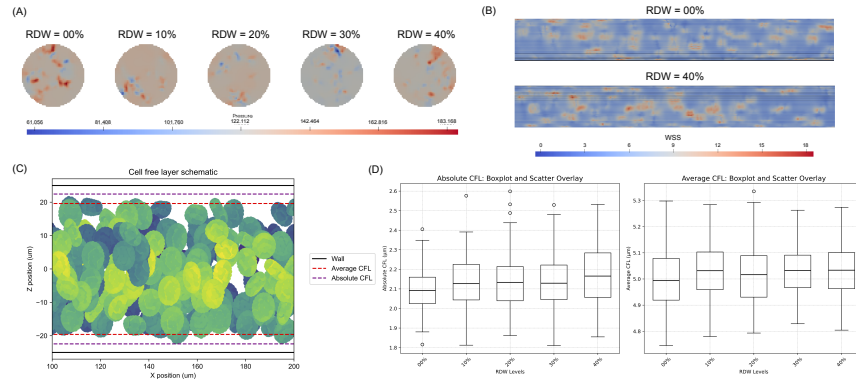


**Fig. 5. Qualitative showcase of hemodynamics and cell transport in cylinder.** (A). Fluid pressure at cross sectional cylinder slice. (B). WSS distribution at RDW = 0% and 40%. (C). Cell-free layer (CFL) width schematic colored by cell velocity. Black line: wall. Red line: Average CFL. Purple line: Absolute CFL. (D). Distribution of average and absolute CFL in the cylinder across different RDW conditions.

To assess the biomechanical impact of RBC heterogeneity, we simulated RBC transport across varying RDW levels in three vascular geometries: a straight cylinder, a bifurcation, and a stenosed vessel. In all cases, the presence of cells perturbed local velocity and pressure fields and generated spatially heterogeneous wall shear stress (WSS) patterns (Figure 5 (A,B)). In the cylinder, RBCs migrated away from the wall, forming a cell-free layer (CFL) (Figure 5 (C,D)). The average CFL width was approximately  $5 \mu\text{m}$ , with minimum widths near  $2 \mu\text{m}$ , consistent with experimental observations [7, 11]. CFL thickness did not differ significantly across RDW conditions, indicating that RBC size heterogeneity does not strongly affect CFL formation under these flow conditions.

In contrast, the bifurcation geometry imposed higher hemodynamic stresses, with flow deceleration and redistribution into daughter branches. Peak fluid pressure reached approximately 400 Pa, compared to 180 Pa in the cylinder, accompanied by elevated cell forces and WSS (Figure 6 (C)). The stenosis produced the most extreme conditions, with marked increases in velocity and pressure at the constriction. Fluid pressure peaked near 2400 Pa in the presence of cells, driving excessive deformation that may compromise cell viability (Figure 6 (D,E)).

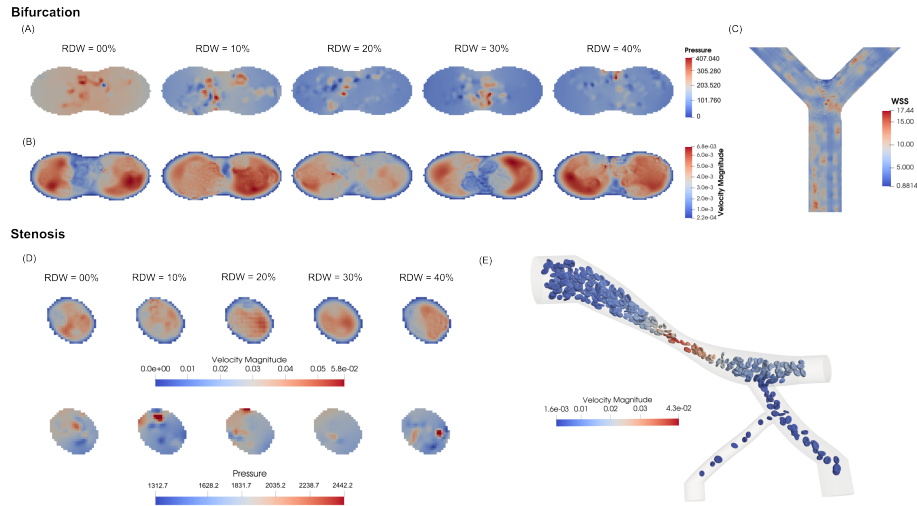


**Fig. 6. Bifurcation and stenosis hemodynamics profile.** Fluid pressure (A) and velocity (B) at cross-sectional bifurcation slice. (C). WSS distribution at RDW = 10% in bifurcation. (D). Fluid velocity and pressure at stenosis cross-sectional slice. (E) RBC dynamics in the stenosis colored by velocity

### 3.2 RBC heterogeneity induces geometry-dependent alterations in cell-scale dynamics while preserving bulk hemodynamics

To further quantify the biomechanical effects of RBC heterogeneity, we analyzed the spatial distributions of key hemodynamic metrics at different levels of RDW. In all geometries, increasing RDW was associated with a consistent increase in fluid velocity median, with the most statistically significant changes observed in the bifurcation model (Figure 7 (A)). This trend likely arises from the disordered packing of heterogeneous RBCs, which creates irregular void spaces and facilitates faster fluid flow compared to uniformly shaped cells. RBCs were more sensitive than the fluid phase to these heterogeneity-driven changes (Figure 7 (B)). The influence of RDW extended to cell velocities and forces, indicating that heterogeneity directly impacts cell dynamics and mechanical load.

In contrast, fluid pressure showed the inverse trend compared to the velocity, where heterogeneity decreased the mean and maximum pressure (Figure 7 (C)). The cylinder experienced a monotonic drop in pressure, whereas the bifurcation first dropped and then increased. Stenosis had the most complicated pattern of going “up-down-up”. Although the magnitudes of the measurements were different in different geometries, the same pattern is true for the maximum shear stress of the wall and the mean cell force between geometries (Figure 7 (D, E)). Significant changes with high percentages of alteration were observed for average cell forces, with great distinction between the homogeneous population and the heterogeneous population. These results suggested that the interplay between RDW and vascular geometry generates emergent biomechanical behaviors that can contribute to disease pathology in a nonlinear manner.

### 3.3 High RDW contributed to increased circulating tumor cell margination

To study the relationship of RDW with cancer metastasis, we also studied the margination behavior of CTCs in an expanded channel (Figure 8 (A)). The trajectories resulted in greater margination over time for higher RDW levels (Figure 8 (B,C)). Due to their high stiffness and material properties, CTCs naturally migrated towards vessel walls, increasing their potential to extravaste and seed metastatic sites [27]. Our simulations revealed that an increase in RDW further enhanced this margination behavior, with the most pronounced effect generating a 221.63% increase in near-wall migration (Table 1). These findings support clinical observations that elevated RDW is associated with a higher metastatic risk with a mechanistic link through enhanced vascular wall interaction of CTCs.

### 3.4 RBC heterogeneity importance for accurate modeling of cell dynamics

While explicitly modeling the heterogeneity of the RBCs offers the highest fidelity, it also incurs a significant computational cost. Our results help identify scenarios in which such detail is necessary versus when a homogeneous approximation may suffice. For simulations focused solely on bulk fluid hemodynamics (e.g., pressure, velocity, and WSS), a homogeneous RBC population can provide accurate results with reduced computational expense. However, when cell-level dynamics are of interest, such as RBC or CTC transport, cell-induced forces, or margination behavior, a heterogeneous model becomes essential. Across multiple geometries, we observed more than 5% differences in cell velocities and forces between homogeneous and heterogeneous populations (Table 1). These deviations are non-negligible for studies concerned with pathophysiological mechanisms, drug delivery, or metastasis modeling. In addition, CTC transport, in particular, requires explicit modeling of RBC heterogeneity to capture the increased margination effects at high RDW, which could influence metastatic seeding and treatment targeting strategies.

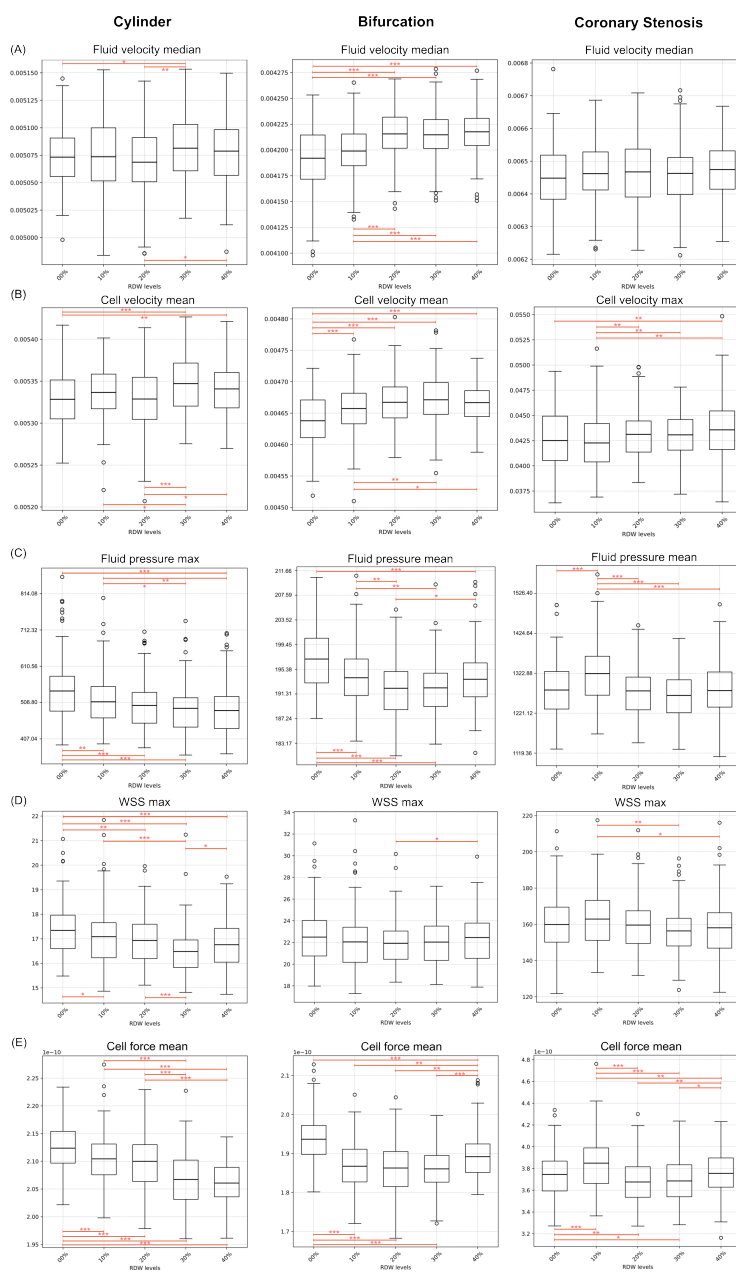


**Fig. 7. Hemodynamics and cell transport alterations.** \*\*\* annotates p-value below 0.001, \*\* below 0.01, and \* below 0.05. **(A).** Fluid velocity (m/s). **(B).** Cell velocity (m/s). **(C).** Fluid pressure (Pascal). **(D).** WSS (Pascal). **(E).** Cell forces (N).

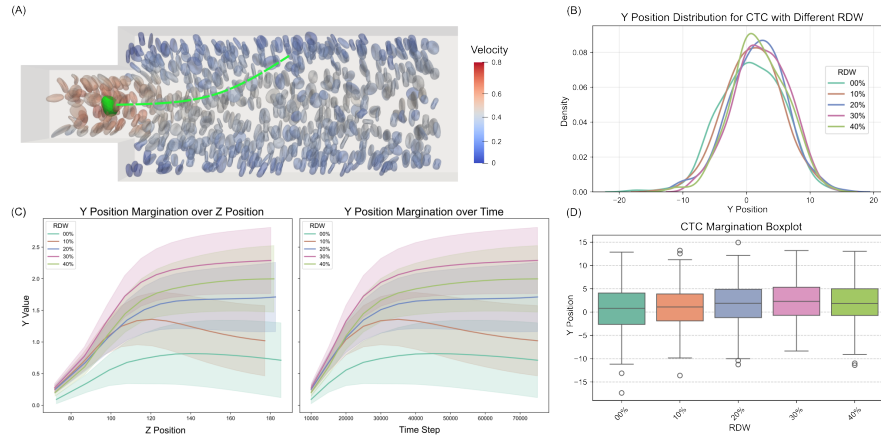


**Fig. 8. CTC margination in the expanded channel. (A).** CTC trajectory tracking (green) surrounded by converged RBCs in the expanded channel. **(B).** KDE plot for end simulation margination position. **(C).** Margination over position and time. **(D).** Boxplot for CTC end simulation margination.

## 4 Conclusion

In this study, we developed and verified a scalable high-resolution fluid-structure interaction framework that explicitly models RBC heterogeneity across clinically relevant RDW ranges. By extending HARVEY with a heterogeneous RBC formulation, we enabled cell-resolved blood flow simulations at scale while preserving numerical accuracy and parallel efficiency. Performance analysis showed that RBC heterogeneity adds minimal computational overhead and no additional scalability bottlenecks, with stable strong and weak scaling confirming that heterogeneous cell populations can be incorporated without compromising performance or numerical stability.

With this simulation platform, we showed that red blood cell heterogeneity induced geometry dependent biomechanical alterations in blood flow and cell transport. Although bulk hemodynamic metrics including velocity, pressure, and wall shear stress remain largely invariant across red blood cell distribution width conditions in simpler geometries, regions of geometric complexity such as bifurcations and stenoses exhibit measurable shifts in local biomechanical profiles. These changes underscore the relevance of red blood cell variability in vascular regions with elevated mechanical stress and pathological susceptibility.

In contrast to bulk flow behavior, cell scale dynamics were strongly modulated by red blood cell distribution width. Variations in red blood cell size distribution significantly affect cell velocity and force generation in a geometry dependent manner. Most notably, circulating tumor cell transport was consistently altered, with elevated red blood cell distribution width producing more than a two fold increase in circulating tumor cell margination toward vessel walls.

**Table 1. RBC heterogeneity affects hemodynamic and cell measurements.** Maximum percentage change reported throughout RDW conditions.

Geometry	Variable	Max Alteration (%)	If Heterogeneity Critical
Cylinder	Fluid pressure	0.02	No
	Fluid velocity	0.04	No
	WSS	4.95	No
	Cell velocity	0.99	No
	Cell force	<b>10.92</b>	Yes
Bifurcation	Fluid pressure	0.03	No
	Fluid velocity	0.72	No
	WSS	2.54	No
	Cell velocity	<b>5.68</b>	Yes
	Cell force	<b>19.4</b>	Yes
Stenosis	Fluid pressure	0.06	No
	Fluid velocity	0.78	No
	WSS	2.22	No
	Cell velocity	1.56	No
	Cell force	<b>5.42</b>	Yes
Expanded channel	CTC margination	<b>221.63</b>	Yes

This finding provided a mechanistic explanation for clinical associations between increased red blood cell distribution width and elevated metastatic risk.

Together, these results demonstrated that homogeneous blood flow models, while adequate for predicting macroscopic hemodynamics, are insufficient for resolving cell level transport phenomena, including margination and cell wall interactions. Future work shall further assess model reliability against experimental benchmarks for key subproblems, including cell free layer formation, red blood cell partitioning in bifurcations, and margination behavior in controlled microfluidic and in vitro flow systems, while also extending the present framework beyond idealized vessel geometries and simplified model assumptions for cell properties. For example, we could characterize additional physiological sources of red blood cell heterogeneity such as membrane stiffness. By providing a flexible and computationally efficient framework, this work established a foundation for future patient specific simulations that integrate red blood cell distribution width with additional biological and geometric factors, enabling more predictive modeling of cardiovascular and oncological disease processes.

## 5 Acknowledgments

This work used Duke Compute Cluster and the Lassen supercomputer at Lawrence Livermore National Laboratory under LLNL Grand Challenges program. Funding was provided by the National Institutes of Health (R01EB024989, DP1AG082343) and the National Science Foundation (1943036). The content does not necessarily represent the official views of the NIH or NSF.

## References

1. Linhui Hu, Manman Li, Yangyang Ding, Lianfang Pu, Jun Liu, Jingxin Xie, Michael Cabanero, Jingrong Li, Ru Xiang, and Shudao Xiong. Prognostic value of RDW in cancers: a systematic review and meta-analysis. *Oncotarget*, 8(9):16027, 2017.
2. Kamil Bujak, Jarosław Wasilewski, Tadeusz Osadnik, Sandra Jonczyk, Aleksandra Kołodziejska, Marek Gierlotka, and Mariusz Gąsior. The prognostic role of red blood cell distribution width in coronary artery disease: a review of the pathophysiology. *Disease markers*, 2015(1):824624, 2015.
3. Dong Xie, Randolph Marks, Mingrui Zhang, Gening Jiang, Aminah Jatoi, Yolanda I Garcés, Aaron Mansfield, Julian Molina, and Ping Yang. Nomograms predict overall survival for patients with small-cell lung cancer incorporating pre-treatment peripheral blood markers. *Journal of Thoracic Oncology*, 10(8):1213–1220, 2015.
4. Noriyuki Hirahara, Yoshitsugu Tajima, Yusuke Fujii, Ryoji Hyakudomi, Tetsu Yamamoto, Kazunari Ishitobi, Takahito Taniura, and Yasunari Kawabata. Prognostic significance of red cell distribution width in esophageal squamous cell carcinoma. *Journal of Surgical Research*, 230:53–60, 2018.
5. Yongping Zhou, Xiding Li, Zhihua Lu, Lei Zhang, and Tu Dai. Prognostic significance of red blood cell distribution width in gastrointestinal cancers: A meta-analysis. *Medicine*, 99(16):e19588, 2020.
6. Lisha Ai, Shidai Mu, and Yu Hu. Prognostic role of RDW in hematological malignancies: a systematic review and meta-analysis. *Cancer cell international*, 18:1–8, 2018.
7. Sharan Ananthaseshan, Krzysztof Bojakowski, Mariusz Sacharczuk, Piotr Poznanski, Dominik S Skiba, Lisa Prahl Wittberg, Jordan McKenzie, Anna Szkulmowska, Niclas Berg, Piotr Andziak, et al. Red blood cell distribution width is associated with increased interactions of blood cells with vascular wall. *Scientific Reports*, 12(1):13676, 2022.
8. Alexis L Caulier and Vijay G Sankaran. Molecular and cellular mechanisms that regulate human erythropoiesis. *Blood, The Journal of the American Society of Hematology*, 139(16):2450–2459, 2022.
9. Nadeeshani Geekiyanage, Emilie Sauret, Suvash Saha, Robert Flower, and Yuan-Tong Gu. Modelling of red blood cell morphological and deformability changes during in-vitro storage. *Applied Sciences*, 10(9):3209, 2020.
10. Anna Bogdanova, Lars Kaestner, Greta Simionato, Amittha Wickrema, and Asya Makhro. Heterogeneity of red blood cells: Causes and consequences. *Frontiers in Physiology*, 11:392, 05 2020.
11. Dmitry A Fedosov, Bruce Caswell, Aleksander S Popel, and George Em Karniadakis. Blood flow and cell-free layer in microvessels. *Microcirculation*, 17(8):615–628, 2010.
12. Alireza Yazdani, Yixiang Deng, He Li, Elahe Javadi, Zhen Li, Safa Jamali, Chensen Lin, Jay D Humphrey, Christos S Mantzoros, and George Em Karniadakis. Integrating blood cell mechanics, platelet adhesive dynamics and coagulation cascade for modelling thrombus formation in normal and diabetic blood. *Journal of the Royal Society Interface*, 18(175):20200834, 2021.
13. Amanda Peters Randles, Vivek Kale, Jeff Hammond, William Gropp, and Efthimios Kaxiras. Performance analysis of the lattice boltzmann model beyond navier-stokes. In *2013 IEEE 27th International Symposium on Parallel and Distributed Processing*, pages 1063–1074, 2013.

14. Claudio Chiastra, Diego Gallo, Paola Tasso, Francesco Iannaccone, Francesco Migliavacca, Jolanda J Wentzel, and Umberto Morbiducci. Healthy and diseased coronary bifurcation geometries influence near-wall and intravascular flow: A computational exploration of the hemodynamic risk. *Journal of Biomechanics*, 58:79–88, 2017.
15. Timm Krüger, Halim Kusumaatmaja, Alexandr Kuzmin, Orest Shardt, Goncalo Silva, and Erlend Magnus Viggen. The lattice Boltzmann method. *Graduate Texts in Physics*, 2017.
16. Monica Diez-Silva, Ming Dao, Jongyoon Han, Chwee-Teck Lim, and Subra Suresh. Shape and biomechanical characteristics of human red blood cells in health and disease. *MRS Bulletin*, 35(5):382–388, 2010.
17. Yasuko Koma, Akira Onishi, Hirofumi Matsuoka, Nao Oda, Naoya Yokota, Yusuke Matsumoto, Midori Koyama, Nobuhiko Okada, Nariyasu Nakashima, Daiki Masuya, Harukazu Yoshimatsu, and Yujiro Suzuki. Increased red blood cell distribution width associates with cancer stage and prognosis in patients with lung cancer. *PLOS ONE*, 8(11):null, 11 2013.
18. E.G. Birgin and R.D. Lobato. A matheuristic approach with nonlinear subproblems for large-scale packing of ellipsoids. *European Journal of Operational Research*, 272(2):447–464, 2019.
19. John Gounley, Erik W Draeger, and Amanda Randles. Numerical simulation of a compound capsule in a constricted microchannel. *Procedia computer science*, 108:175–184, 2017.
20. Charles S Peskin. The immersed boundary method. *Acta numerica*, 11:479–517, 2002.
21. Sayan Roychowdhury, Erik W Draeger, and Amanda Randles. Establishing metrics to quantify underlying structure in vascular red blood cell distributions. In *International Conference on Computational Science*, pages 89–102. Springer, 2022.
22. Madhurima Vardhan, Cyrus Tanade, S. James Chen, Owais Mahmood, Jaidip Chakravartti, W. Schuyler Jones, Andrew M. Kahn, Sreekanth Vemulapalli, Manesh Patel, Jane A. Leopold, and Amanda. Randles. Diagnostic performance of coronary angiography derived computational fractional flow reserve. *Journal of the American Heart Association*, 2024.
23. WF Hynes, M Pepona, C Robertson, J Alvarado, K Dubbin, M Triplett, JJ Adorno, A Randles, and Monica L Moya. Examining metastatic behavior within 3D bio-printed vasculature for the validation of a 3D computational flow model. *Science advances*, 6(35):eabb3308, 2020.
24. John Gounley, Rafeed Chaudhury, Madhurima Vardhan, Michael Driscoll, Girish Pathangey, Kevin Winarta, Justin Ryan, David Frakes, and Amanda Randles. Does the degree of coarctation of the aorta influence wall shear stress focal heterogeneity? In *2016 38th annual international conference of the IEEE Engineering in Medicine and Biology Society (EMBC)*, pages 3429–3432. IEEE, 2016.
25. Peter Balogh, John Gounley, Sayan Roychowdhury, and Amanda Randles. A data-driven approach to modeling cancer cell mechanics during microcirculatory transport. *Scientific reports*, 11(1):15232, 2021.
26. Junyu Nan, Sayan Roychowdhury, and Amanda Randles. Investigating the influence of heterogeneity within cell types on microvessel network transport. *Cellular and Molecular Bioengineering*, 16(5):497–507, 2023.
27. Sayan Roychowdhury, John Gounley, and Amanda Randles. Evaluating the influence of hemorheological parameters on circulating tumor cell trajectory and simulation time. In *Proceedings of the Platform for Advanced Scientific Computing Conference*, pages 1–10, 2020.